Detection and classification of Real Time Power Quality Disturbance Signals with HMMs incorporating with SGWT Features

S. Upadhyaya

Department of Electrical Engineering, SUIIT, Burla,
Sambalpur India

***Abstract*: In this paper, Second generation Wavelet Transform (SGWT) has been implemented along with the traditional discrete Wavelet Transform (DWT) for localization of different types of power quality (PQ) disturbance signals. Selected features have been extracted from the detail coefficient of the variants of WT and then fed as inputs to the classifiers in order to characterize the signals. Moreover, a comparative assessment of the PQ signal carried out with Multilayer perceptron (MLP) and Hidden Markov Models (HMMs). For localisation of power quality disturbances, the signals have been analysed upto four decomposition levels whereas for classification the signals are decomposed for seven decomposition levels. In order to represent in realistic environment, these proposed techniques are tested with the signals captured from transmission line panels. Further, to aid these PQ disturbance detection, different types of real time fault signals are also characterized with these aforementioned approaches.**

I. INTRODUCTION

The Power Quality disturbance (PQD) study has become an emerging issue in the area of power system, as the disturbances affect the overall harmony of the system. The proper and the continuous monitoring of the power quality disturbances has become a significant issue both for the utilities and the end-users. The operation of the power system can be improved by analyzing the PQ disturbances consistently. Hence, the development of the techniques and the methodologies in order to diagnose the power quality disturbances has become an importance issue in research. The PQ is actually the combination of quality of the voltage and the quality of current [1], [2] but in most of the cases, it is generous with the quality of voltage as the power system can only control the voltage quality. Hence, the yardstick of the power quality area is to preserve the supply voltage within the tolerable limits [3], [4]. The maintenance of quality of power in terms of voltage requires proper selection of the suitable detection and the characterisation methods. These are the crucial steps to maintain the healthy power system by mitigating the PQ disturbances.

In order to identify the disturbances, the different techniques such as the Fourier transform (FT), the short-time Fourier transform (STFT), wavelet transform (WT), Neural Network, Fuzzy logic, S-transform have been used [5], [6]. The FT is a fast technique which only provides the information about the frequency component and does not give any information about time. The time frequency information related to the disturbance waveform can be obtained in STFT [7]. However, STFT is unsuitable to track the transient signals perfectly due to its fixed window property [8]. Similarly, the S-transform suffers from computational burden which limits its applications [9]. The wavelet transform affords the time-scale analysis of the non-stationary signal due to Multi-Resolution Analysis (MRA) property. The property of MRA of WT represents the signals into different time-scales rather than the time-frequency. Thus, WT is a suitable technique for analysis of the transient signals as it provides long window at low frequencies and short window at high frequencies [10].

The time plays an important role in the power system operation. One of the important issues of PQ problem is the fast mitigation of the disturbances. Fast detection and localization of the disturbances promote the fast mitigation. In other words, the fast detection of PQ disturbance is becoming an important factor in deregulated market. Both, Discrete Wavelet Transform(DWT) and Second Generation Wavelet Transform(SGWT) decomposition techniques are applied to detect and localise the different types of power quality disturbances.

The accurate detection of the PQ disturbance is the important performance indices in power quality analysis. The automatic detection of PQ events with the discrete wavelet transform (DWT) is a common topic in past studies [11], [12]. The time plays an important role in the power system operation. One of the important issues of PQ problem is the fast mitigation of the disturbances. Fast detection and localization of the disturbances promote the fast mitigation. In other words, the fast detection of PQ disturbance is becoming an important factor in deregulated market. Both, Discrete Wavelet Transform (DWT) and Second Generation Wavelet Transform (SGWT) decomposition techniques are applied to detect and localise the different types of power quality disturbances.

In order to reduce the memory consumption, the features has been extracted from the detail coefficients of the WT decomposition instead of giving the raw data directly. In this paper, the traditional DWT and the SGWT are integrated with the feature extraction [13], [14] of PQD signals which is followed by classification. The Multilayer perceptron (MLP) and the Hidden Markov Models (HMMs) have been implemented to classify the PQD signals.

This paper organized as follows. The Section-II describes the theory of the Second Generation Wavelet Transform (SGWT) along with the Discrete Wavelet transform (DWT). The feature extraction processes are presented in the Section-III. Section-IV provides the brief theory about the classifiers. Similarly, the Section-V deals with the construction of PQ model as well as the effectiveness of SGWT and DWT in the localization of the PQ disturbances. The classification results are presented in the Section-VII. Finally, Section-VIII provides the concluding remark.

II. LOCALIZATION APPROACH

The basic block diagram of the classification of PQ signals which is preceded by decomposition and feature extraction. The detection of the PQ disturbance has been carried out with the help of DWT and SGWT. These have been described briefly in this section while the feature extraction and classification are described in the subsequent sections.

A. Continuous Wavelet Transform

The wavelet transform represents the signal as a combination of the wavelets at different location (position or amplitude) and scales (duration or time). The continuous wavelet transform generally implements for the continuous time signal analysis. The surface of the wavelet coefficients has been obtained from the different values of the scaling and the translation factors.

Mathematically, for a signal $x(t)$, the continuous wavelet transform [15] is expressed as

$$CWT(a,b) = \frac{1}{\sqrt{a}} \int_{-\infty}^{\infty} x(t) g\left(\frac{t-b}{a}\right) dt \tag{1}$$

where $g(\cdot)$ is the mother wavelet. Similarly, a is the scale factor and b is the translation factor. Both a and b are varies in continuous manner in continuous wavelet transform . In order to remove the redundancy due to continuous coefficients, discrete Wavelet transform has been introduced which has been discussed in next subsequent subsection.

B. Discrete Wavelet Transform

The discrete wavelet transform (DWT) implements in order to decompose a discretized signal into different resolution levels. The DWT reduces the substantial redundancy of CWT. In the multiresolution analysis (MRA), the wavelet function generates the detail coefficients of the decomposed signal and the scaling function generates the approximation coefficients of the decomposed signal. The DWT can be expressed with g as the mother wavelet

$$DWT(m,k) \frac{1}{\sqrt{a_0^m}} \sum_n x(n) g\left(\frac{k - n b_0 a_0^m}{a_0^m}\right) \tag{2}$$

where k is an integer. The scaling parameter and translation parameter a and b vary in the discrete manner. The time signal $S[n]$ decomposed in to detailed $d_1(n)$ and smoothed $c_1(n)$ employing high pass ($h(n)$) and low pass filters ($l(n)$). Thus the detail version contains high frequency components than the smooth version $c_1(n)$. Mathematically, they are specified [16] as

$$c_1 = \sum_k h(k-2n) c_0(k) \tag{3}$$

$$d_1(n) = \sum_k g(k-2n) c_0(k) \tag{4}$$

where $c_0(n)$ is the discretised time signal (sampled version of $S_0(n)$). The outputs of the two filters are down sampled by a factor of 2 in order to obtain the DWT coefficients. The output of the low pass filter is called the approximation coefficients and the output of the high pass filter is called as the detail coefficients. The approximation coefficients are further fed to the low pass and high pass filter and the process is repeated. The high pass and low pass filters are called as the 'Quadrature mirror filters' and are related by the equation

$$h[L-1-n] = (-1)^n l(n) \tag{5}$$

where, L is the length of filter. The basic block diagram of DWT is shown in Fig.1.

As DWT is frequency domain analysis, it requires more time than the time domain analysis. The Second Generation Wavelet Transform (SGWT) overcomes the drawbacks of the DWT which is presented in the subsequent subsection.

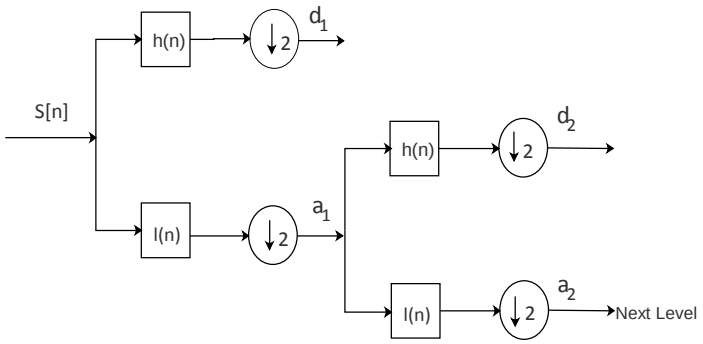

Fig. 1: Block diagram of DWT decomposition

C. Second Generation Wavelet Transform

The second generation Wavelet Transform (SGWT) is the variant of WT. The Lifting scheme (LS) based SGWT is similar to the traditional DWT. The SGWT consists of the iterations of the three operations as split, predict and update [**?**], [**?**], [**?**] as shown in Fig.2.

- **Split**: In the analysis of SGWT, first the signal $S[n]$ is divided into two disjoint subsets as the even index set $X[n]_{even}$ and the odd index set $Y[n]_{odd}$, which are correlated. This local correlation structure has the ability to predict and the update is described below.

$$S[n] = X[n]_{even} + Y[n]_{odd} \quad (6)$$

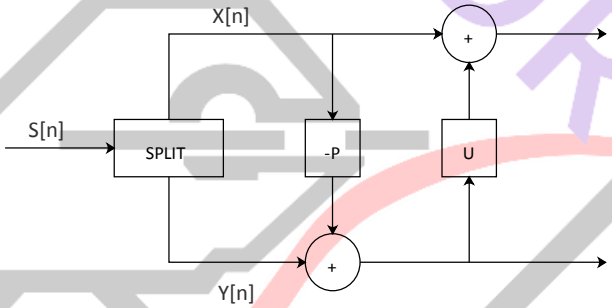

Fig. 2: Block diagram representation of SGWT decomposition

- **Predict** : The details of the original signal $S[n]$ are determined in this step using the wavelet decomposition as given in (7). Using the predictor operator P, $Y[n]$ is predicted from $X[n]$.

$$d[n] = Y[n] - P(X[n]) \quad (7)$$

- **Update** : The approximation coefficients of the original signal $S[n]$ are determined by using (8). The update operator U is applied to the details and the result is added with $X[n]$ in this step.

$$C[n] = X[n] + U(d[n]) \quad (8)$$

The process is further iterate with the approximation generated at the first level.

III. THEORY OF THE FEATURE EXTRACTION

A. Feature extraction

The input to the classifiers has been extracted features from the output of the signal decomposition instead of directly using the raw data in ordered to reduce the computational burden. The quantitative analysis in terms of features like the energy content, the standard deviation (STD), the cumulative sum (CUSUM) and the entropy of the transformed signal has been performed to reduce the classification error. The basis of choosing the features has been explained below along with the proper expressions [14].

- **Energy** : According to Parseval's theorem the energy of the distorted signal will be partitioned at different resolution levels in different ways depending on the power quality disturbances signals. So, it has been established that energy distribution pattern changes when the amplitude and frequency of the signal changes [17] and [5].

$$\text{Energy } ED_i = \frac{1}{N}\sum_{j=1}^{N}\left|D_{ij}\right|^2 \tag{9}$$

where i = 1,2,3,...,l (level of decomposition) and N is the number of samples in each decomposed data. D stands for detail coefficient.

- **Entropy** : The spectral entropy of the non-stationary power signal disturbances is an effective parameter for the classification of the signal. The entropy value for low frequency disturbances like the voltage swell, the voltage sag, the momentary interruption and the pure undistorted sinusoidal signal is minimum. The harmonics contained in the signals such as sag with harmonics, swell with harmonics have a comparatively high entropy value. For flicker type signals the entropy value is minimum. Similarly in case of the short duration non-stationary power signal disturbances such as the notches and the spikes have very low entropy values. While transients have relatively higher entropy value [8].

$$\text{Entropy } ENT_i = -\sum_{j=1}^{N} D_{ij}^2 \log(D_{ij}^2) \tag{10}$$

- **Standard deviation** : Assuming a zero mean, the standard deviation can be considered as a measure of the energy of the considered signal. Standard deviation has been employed to differentiate the low frequency and the high frequency signals [5].

$$\text{Standard Deviation } \sigma_i = \left(\frac{1}{N}\sum_{j=1}^{N}(D_{ij}-\mu_i)^2\right)^{\frac{1}{2}} \tag{11}$$

- **CUSUM** : The cumulative sum method implements the samples for the localization of the distortion in the signal. The CUSUM has been computed by the sum of the consecutive samples of the power quality signal after being passed through the aforementioned transforms [18].

$$\text{CUSUM } CM_i = \sum_{j=1}^{N}(D_{ij}-\mu_i)^2 \tag{12}$$

where Mean $\mu_i = \frac{1}{N}\sum_{j=1}^{N} D_{ij}$

These four features have been extracted from the output of the transformation. At each level four features have been extracted, so for each signal in WT $4 * 7$ feature vector have been formed. After calculating the features for the complete data sets, the feature vectors are normalised between [0,1] by considering the maximum value of the corresponding feature vectors as the base. However, the normalisation is one of the important steps of pre processing of the data before classification. This vector normalisation has been carried out in order to avoid the influence of high range feature vectors over low range ones. The extracted features have been fed as put to the classifiers.

IV. CLASSIFICATION APPROACH

The extracted features are fed as inputs to the classifier such as MLP and HMMs.

A. Hidden Markov models (HMMs)

The HMMs have been applied to feature vector extracted from the coefficient in order to determine the maximum likelihood in the data set. The HMM, extension of the Markov model in which the stochastic process is not directly observable through another set of stochastic processes. However, an HMM can be defined as $\lambda = (M,N,\pi,A,B)$ where the parameter N denotes the number of states of the model, M is the number of distinct observation symbols per state, π is the initial state distribution vector, similarly , A denotes the state transition probability and finally B is observation probability matrices respectively. A discrete HMM is explained in [15], [8] through the model of individual states. Like other classifiers, the HMMs operation has been partitioned into the training and the testing stage of dataset. The HMM training model uses both continuous and discrete density modelling and also employs the Baum-Welch algorithm to construct the HMMs [19], [20], [21].

PQD events	Class
Sag	*CL*1
Swell	*CL*2
Interruption	*CL*3
Oscillatory transient	*CL*4
Flicker	*CL*5
Harmonics	*CL*6
Sag + Harmonics	*CL*7
Swell + Harmonics	*CL*8
Notch	*CL*9
Spike	*CL*10

Starting with a very simple prototype system, the HMMs are repeatedly modified and re-estimated until the required level of model complexity and performance is reached. In this study, ten different HMMs has been trained for ten different disturbance classes. For this classification process, the logarithmic probability of each model output has been determined for the unknown input signals. In order to develop a proper HMM, the selection of the optimum number of state and the density function are very important but there is no explicit rule for the selection of these factors except the application TABLE I: Power signal Class labels of synthesis signal type and the parameters. In this work, three states has been selected to stipulate the output with the Gaussian mixtures function. The prior distribution has been used over the state transition to favour the transitions in order to stay in the same state. The prior is multiplied by the likelihood function and then normalised according to the Bayes theorem. The CA depends on the number of matching of the testing with the trained model using the equation.

V. POWER QUALITY DISTURBANCE MODEL

The theory described in Section-II has been used to compute the approximation and detail coefficients up to fourth finer levels using the DWT and SGWT. The PQD signals are simulated in MATLAB with sampling frequency is 3.2 kHz [22]. Class labels assigned to PQ signals of synthesized signals are given in Table I.

VI. DECOMPOSITION OF PQ SIGNALS

A. Pure Sinusoidal Voltage Signal

A sinusoidal voltage signal is considered in Fig.3. Using DWT and SGWT the signals are decomposed up to four decomposition levels which are shown in Fig.3 along with the original sine wave. The horizontal axis represents time in second in terms of samples and the vertical axis represents the amplitude of voltage signal in volt (V). Both DWT and SGWT has been implemented on the aforementioned PQ signals in order to carry out the analysis. Using the DWT and the SGWT decomposition, similar types of waveforms are produced at the respective decomposition level along with the original waveform. The decomposition levels and

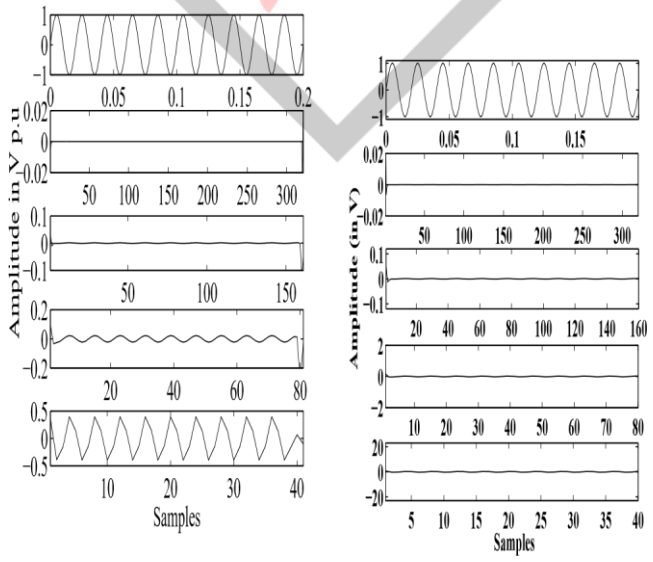

(a) (b)

Fig. 3: Localization of pure sine wave in (a) DWT decomposition (b) SGWT decomposition

the corresponding description of the pure sine wave with sag and swell are shown in Fig.4 and Fig. 5 respectively.

B. Pure sine wave with sag

A sinusoidal voltage signal with the sag is decomposed up to four levels using DWT and SGWT. These levels are shown in Fig.4. Similar types of waveform at the respective decomposition levels are produced in both the decomposition methods. The horizontal axis represents the samples and the vertical axis represents amplitude in volt in per unit. The point of sag can be observed at each decomposition level with both the methods. Similarly, the starting and end points of the disturbance of each decomposition levels are in the same alignment with the original signal in both DWT and SGWT.

From the Fig.4 it is observed that, both the DWT and the SGWT decomposition have given similar type of waveforms in respective decomposition levels.

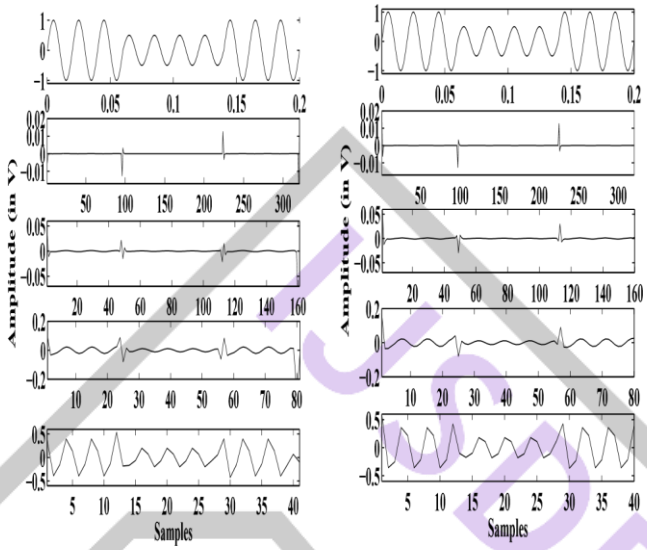

(a) (b)

Fig. 4: Localization of sine wave with sag in (a) DWT decomposition (b) SGWT decomposition

C. Pure sine wave with swell

The procedure adopted is the same as the above case. In Fig.5, similar types of waveforms are found in the same decomposition levels.

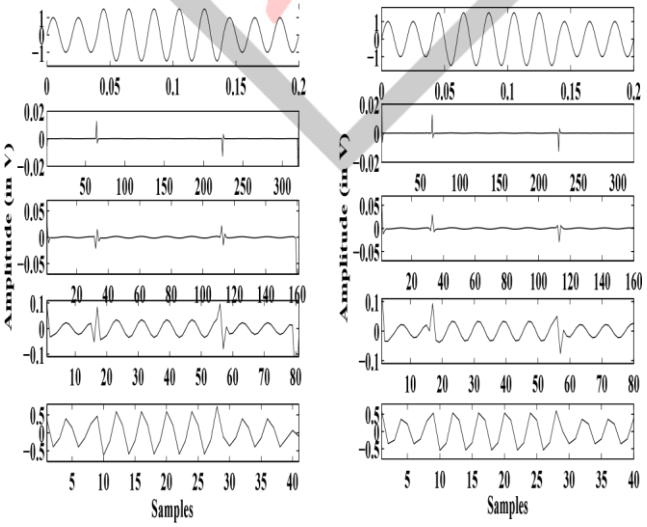

(a) (b)

Fig. 5: Localization of sine wave with swell in (a) DWT decomposition (b) SGWT decomposition

Similarly, the rest PQ disturbances are subjected to the process of decomposition using the DWT and the SWGT. Similar types of waveforms are obtained from both types of wavelet transforms.

D. Harmonic voltage signal

Consider the harmonic signal shown in Fig.6. By observing 1st two levels of Fig.3 and Fig.6, it can be observed that for sinusoidal signal the magnitude of 1st two levels are almost zero and for harmonic signal, 1st two levels have some magnitude. Hence, it can be concluded that the waveforms of each level are different for different disturbance and this property helps in classification of those disturbances.

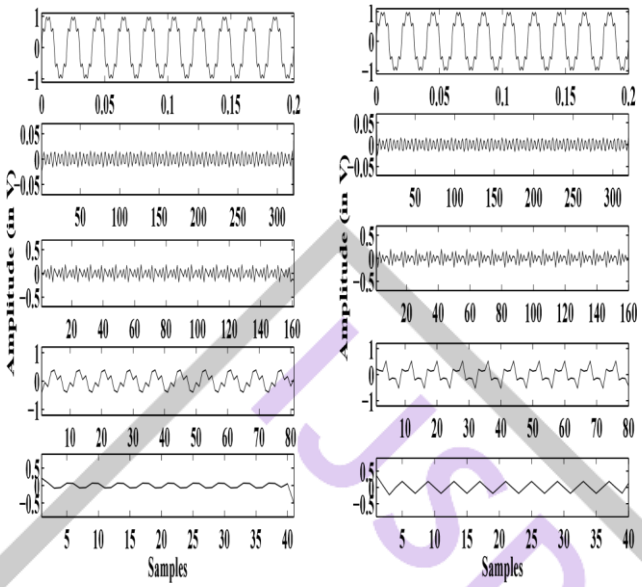

(a) (b)

Fig. 6: Sine wave with Harmonic (a) DWT decomposition (b) SGWT decomposition

E. Pure sine wave with harmonic and sag

The distortions are detected and localized in the finer levels of DWT and SGWT decomposition shown in Fig.7. By observing 1st two levels of Fig.4 and Fig.7, it can be observed that for sinusoidal signal with sag, the magnitude of 1st two levels are almost zero

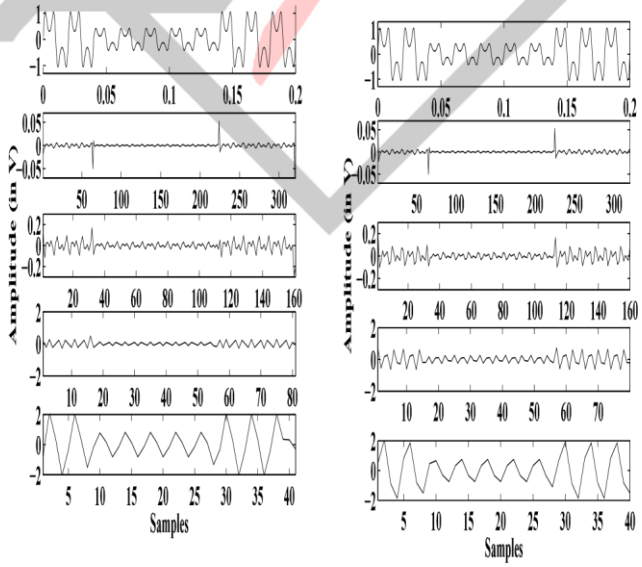

(a) (b)

Fig. 7: Sine wave with Harmonic and sag (a) DWT decomposition (b) SGWT decomposition

except the occurrence and end point of disturbance and for harmonic signal, 1st two levels have some magnitude. Hence, it can be concluded that the waveforms of each level are different for different disturbance and this property helps in classification of those disturbances. At same decomposition level, both DWT and SGWT show the same type of waveforms.

F. Pure sine wave with notch

A pure sine wave with notch is taken in consideration. The notches are clearly detected and localized in the finer levels of DWT and SGWT decomposition shown in Fig.8.

Waveforms found in both SGWT and DWT are similar at the same decomposition levels. However SGWT is faster than the traditional DWT.

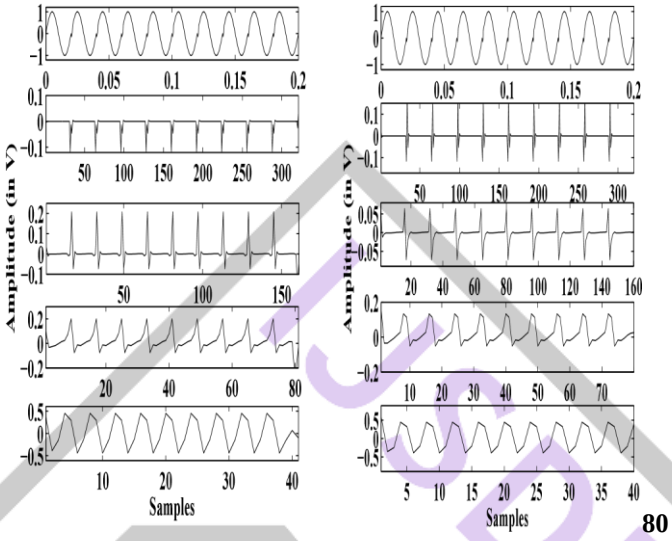

Fig. 8: Sine wave with notch (a) DWT decomposition (b) SGWT decomposition

. G. Experimental PQD Signal generation

In order to get the real data, seven types of PQ signals have been generated by employing transmission line panel, the load and the storage oscilloscope.

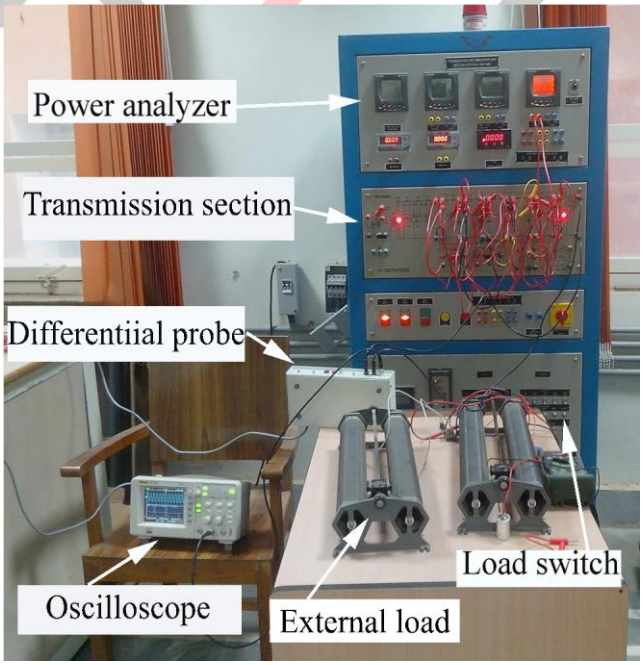

Fig. 9: Experimental setup for single phase voltage signal collection

The transmission demo panel comprises a line model with the length 400 Km and voltage of 220 kV. The lumped parameter line model with five cascaded networks each of them has been designed for 80 km parameters. The fault simulating switch has been provided to create the fault condition. This transmission line panel also comprises digital DSP based power analysers, voltmeters, ammeters, push buttons, indicating lamp and a digital timer is also present. The demo panel is also provided with protective devices i.e MCB'S to give protection from any abnormal condition occurring during the actual demonstration and experiments. The numerical impedance relay and the numerical over current relay are also associated to give trip signal to the circuit breaker. The current carrying capacity of the model is 5 Amp.

The seven types of signals are sag, swell, interruption, sag with swell, sag with interruption, swell with interruption and sag and swell with interruption. A 220 V is applied to the transmission line panel and by changing the load and creating fault, the various disturbances are created. The disturbances are then stored in storage oscilloscope. Then data is extracted from the oscilloscope and fed to the MATLAB for feature extraction and subsequent classification. The details of experimental set up is given in Fig.9. Similarly, the circuit diagram of the transmission panel has been shown in Fig.10. The captured single phase voltage signals with sag, swell and interruption are presented in Fig.11.

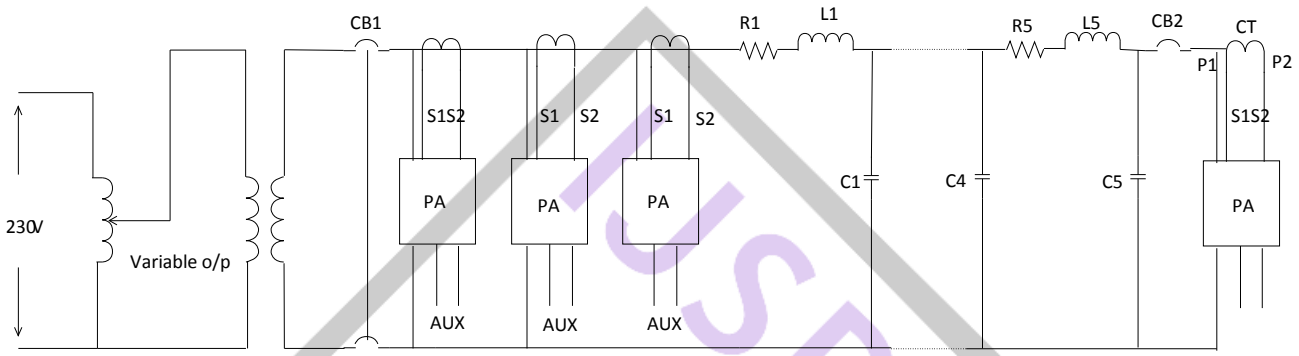

Fig. 10: Circuit diagram of the single phase transmission panel connection

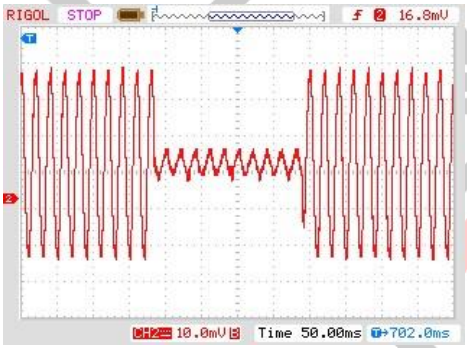

(a) Voltage with sag

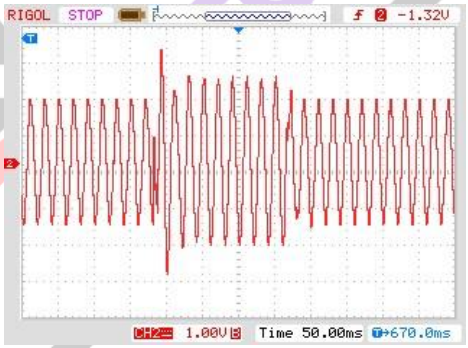

(b) Voltage with swell

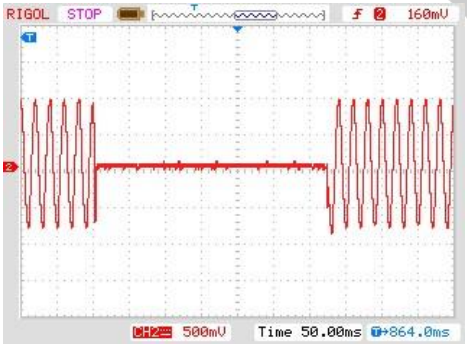

(c) Voltage with interruption

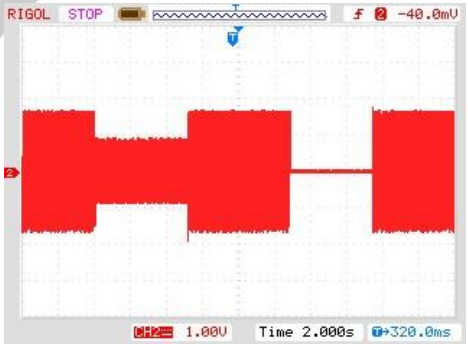

(d) Voltage with interruption and sag

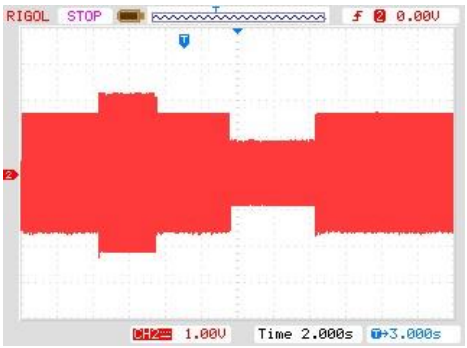

(e) Voltage with sag and swell

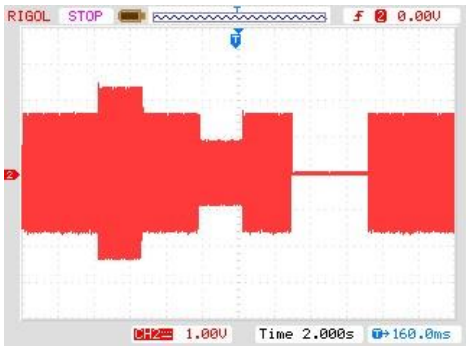

(f) Voltage with sag, swell and interruption

Fig. 11: Single phase real voltage signals with disturbances

VII. CLASSIFICATION RESULTS

A. Classification with simulated PQD signals

The classification accuracy is computed by the automated classifiers described in Section-III. The total 10936 numbers PQD signals are simulated with MATLAB. Each data set contains variable X ($X1-$ standard deviation, $X2-$ energy of details, $X3-$ entropy, $X4-$CUSUM) and $L(L1,L2,...,L7$ level of decomposition) which constitute 28 features. For each classifier 70% of the total data has been treated as the training data and the rest 30% data are employing for the testing.

For ten different types of disturbances the overall classification accuracy (%CA) is also calculated individually. The classification accuracy is a measure of the performance index of the PQ defined [23] as

$$Classification\ Accuracy(\%) = \frac{Number\ of\ \ samples\ correctly\ classified}{Tota\ number\ of\ \ samples\ in\ the\ class} \times 100 \quad (13)$$

In the Table II, the (*CA*%) of MLP and HMMs classifiers also have been presented. From, Table II, it has been observed that for each data set the overall (*CA*%) of MLP is better than the HHMs as it fails to classify interruption, harmonic like slow disturbances. When we observe the individual (*CA*%), the HMMs has better (*CA*%) than the MLP in case of fast signals like transient, notch and spike etc.

The classification of three phase PQ disturbances have been presented in Table III. From Table III, it can be observed that %*CA* value of three phase signals are similar to the synthetic signal %*CA* value. The SGWT requires a half number of computations as compared to the traditional convolution based DWT, in which computation of SGWT is faster than DWT. From these above tables, it is observed that though the DWT based data set has similar classification accuracy that of the SGWT but processing time of SGWT is lesser than the DWT. Similarly, the auxiliary memory consumption of SGWT is reduced as compared to DWT as the lifting scheme based on SGWT, allows a fully in-place calculation of WT.

TABLE II: CA (%) of Pure Signals

CLASS	DWT		SGWT	
	MLP	HMMs	MLP	HMMs
CL1	86.56	76.21	88.99	77.09
CL2	86.96	98.32	88.21	98.34
CL3	90.01	0	90.98	0
CL4	89.94	98.01	91.12	98.45
CL5	87.79	92.01	88.02	93.12
CL6	91.11	47.61	92.67	48.63
CL7	87.34	43.32	89.36	44.78
CL8	88.47	73.60	90.67	74.37
CL9	90.34	100	91.02	100
CL10	89.07	98.02	91.13	98.45
TOTAL %CA	89.82	71.02	90.89	72.32

Similarly, the aforementioned proposed methods have also been implemented on fault classification in order to check suitability of these methods.

TABLE III: CA (%) of real time single phase signals

CLASS	DWT		SGWT	
	MLP	HMMs	MLP	HMMs
C1	82.56	72.36	84.69	79.04
C2	83.36	92.47	84.87	99.02
C3	87.21	0	85.64	0
C1+C2	85.34	88.34	86.58	89.02
C1+C3	84.39	13.01	86.94	16.03
C2+C3	83.16	47.61	85.02	50.06
C1+C2 +C3	84.34	43.32	86.02	46.06
TOTAL %CA	84.21	60.34	86.98	63.46

B. Fault Classification

Under normal operating condition, the power system operates under balanced conditions with all the equipments carrying normal currents and voltages within the prescribed limits.

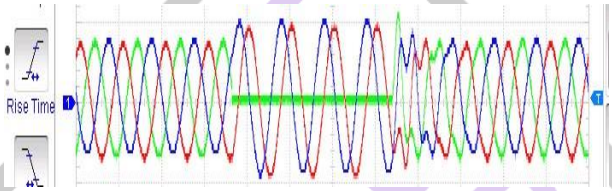

(a) L–G fault

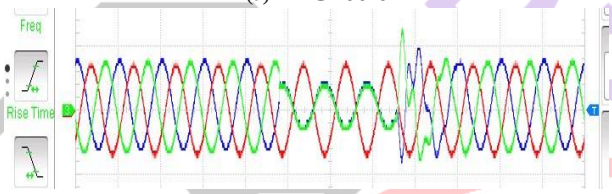

(b) L–L fault

(c) L-L-G fault

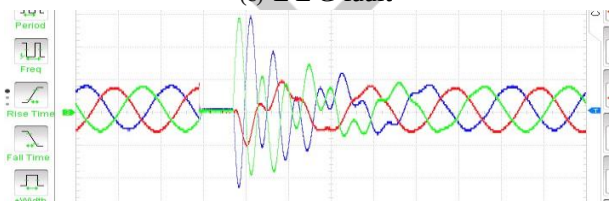

(d) L-L-L-G fault

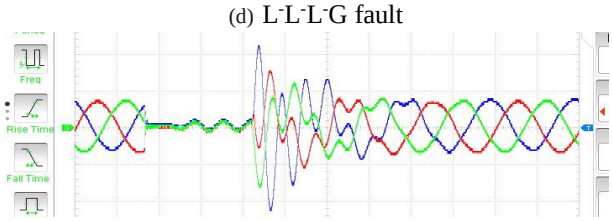

(e) L-L-L fault

Fig. 12: Three phase real voltage signals fault

This healthy operating condition can be disrupted due to a fault in the system. The power system faults are divided in to three phase balanced fault and unbalanced fault. The different types of unbalanced fault are single line to ground fault (L−G), line to line fault (L−L), double line to ground (L−L−G). The balanced faults are three phase fault which are severe type of fault. These faults can be two types such as line to line to line to ground (L−L−L−G) and line to line to line fault (L−L−L).

TABLE IV: CA (%) of three phase fault signals

CLASS	DWT		SGWT	
	MLP	HMMs	MLP	HMMs
L−G	75.21	80.0	82.00	84.00
L−L	83.76	78.76	82.01	82.52
L−L−G	86.75	88.33	81.82	83.52
L−L−L−G	74.14	81.17	85.33	89.05
L−L−L	91.42	91.94	88.63	90.25
TOTAL %CA	83.51	85.42	87.35	89.92

Three phase voltage signals with fault are captured from an overhead π modelled transmission line of length 360 (Km) like the other cases. Total five types of fault signals are captured from a three phase transmission line panel. Some of fault signals have been presented in Fig.12. Fault signals have been captured from the oscilloscope and fed to MATLAB for analysis like the previous cases. From the details of the WT four features have been extracted and fed to the classifiers in order to recognise the type of fault. The recognition rate in terms of %*CA* is given in Table IV.

Different approaches have been implemented for calculation of %*CA* in Table IV. From these tables, it can be observed that all the aforementioned techniques are working satisfactorily. The HMMs have provided good results unlike the PQ disturbance recognition where it failed to recognise slow disturbances perfectly. In case of fault classification, HMMs have been provided satisfactory result for both overall %*CA* as well as individual %*CA*.

VIII. CONCLUSION

The useful features of the PQD signals have been extracted using the DWT and the SGWT. The classification accuracy of simulated and real signals are obtained by SGWT as well as DWT, combined with MLP and HMMs. From these aforementioned classifiers it is observed that though DWT has yielded, similar classification accuracy like the SGWT. In other words, the SGWT is simple, robust and suitable for single as well as combined disturbances. An intensive comparative assessment in terms of classification accuracy also leads to conclude that the suitability of SGWT is better than convolution based DWT. The main disadvantage of MLP is the requirement of retraining when a new phenomenon is added.Moreover, the HMMs have provided satisfactory result for fast signals like transient spike etc as well as transmission line fault signals. So HMMs are classifiers for classification of fast signals.

REFERENCES

[1] M. Bollen, “What is power quality?,” *Electric Power Systems Research*, vol. 66, no. 1, pp. 5–14, 2003.

[2] P. Janik and T. Lobos, “Automated classification of power-quality disturbances using svm and rbf networks,” *IEEE Transactions on Power Delivery*, vol. 21, no. 3, pp. 1663–1669, 2006.

[3] S. Khokhar, A. Mohd Zin, A. Mokhtar, and N. Ismail, “Matlab/simulink based modeling and simulation of power quality disturbances,” in *IEEE Conference on Energy Conversion (CENCON)*, pp. 445–450, IEEE, 2014.

[4] D. O. Koval, “Power system disturbance patterns,” *IEEE Transactions on Industry Applications*, vol. 26, no. 3, pp. 556–562, 1990.

[5] A. Gaouda, M. Salama, M. Sultan, and A. Chikhani, “Power quality detection and classification using wavelet-multiresolution signal decomposition,” *IEEE Transactions on Power Delivery*, vol. 14, no. 4, pp. 1469–1476, 1999.

[6] L. Angrisani, P. Daponte, M. D’apuzzo, and A. Testa, “A measurement method based on the wavelet transform for power quality analysis,” *Power Delivery, IEEE Transactions on*, vol. 13, no. 4, pp. 990–998, 1998.

[7] D. Gabor, “Theory of communication. part 1: The analysis of information,” *Journal of the Institution of Electrical Engineers-Part III: Radio and Communication Engineering*, vol. 93, no. 26, pp. 429–441, 1946.

[8] B. Biswal, M. Biswal, S. Mishra, and R. Jalaja, “Automatic classification of power quality events using balanced neural tree,” *Industrial Electronics, IEEE Transactions on*, vol. 61, no. 1, pp. 521–530, 2014.

[9] R. A. Brown and R. Frayne, “A fast discrete s-transform for biomedical signal processing,” in *Engineering in Medicine and Biology Society, 2008. EMBS 2008. 30th Annual International Conference of the IEEE*, pp. 2586–2589, IEEE, 2008.

[10] I. Daubechies, “Orthonormal bases of compactly supported wavelets,” *Communications on pure and applied mathematics*, vol. 41, no. 7, pp. 909–996, 1988.

[11] A. G. Hafez, E. Ghamry, H. Yayama, and K. Yumoto, "A wavelet spectral analysis technique for automatic detection of geomagnetic sudden commencements," *Geoscience and Remote Sensing, IEEE Transactions on*, vol. 50, no. 11, pp. 4503–4512, 2012.

[12] D. B. Percival and A. T. Walden, "Wavelet methods for time series analysis (cambridge series in statistical and probabilistic mathematics)," 2000.

[13] C.-Y. Lee and Y.-X. Shen, "Optimal feature selection for power-quality disturbances classification," *Power Delivery, IEEE Transactions on*, vol. 26, no. 4, pp. 2342–2351, 2011.

[14] B. Panigrahi and V. R. Pandi, "Optimal feature selection for classification of power quality disturbances using wavelet packet-based fuzzy k-nearest neighbour algorithm," *IET generation, transmission & distribution*, vol. 3, no. 3, pp. 296–306, 2009.

[15] S. Santoso, E. J. Powers, W. M. Grady, and P. Hofmann, "Power quality assessment via wavelet transform analysis," *Power Delivery, IEEE Transactions on*, vol. 11, no. 2, pp. 924–930, 1996.

[16] C. H. Kim and R. Aggarwal, "Wavelet transforms in power systems. i. general introduction to the wavelet transforms," *Power Engineering Journal*, vol. 14, no. 2, pp. 81–87, 2000.

[17] T. Zhu, S. Tso, and K. Lo, "Wavelet-based fuzzy reasoning approach to power-quality disturbance recognition," *Power Delivery, IEEE Transactions on*, vol. 19, no. 4, pp. 1928–1935, 2004.

[18] S. Mohanty, A. Pradhan, and A. Routray, "A cumulative sum-based fault detector for power system relaying application," *IEEE Transactions on Power Delivery*, vol. 23, no. 1, pp. 79–86, 2008.

[19] L. R. Rabiner, "A tutorial on hidden markov models and selected applications in speech recognition," *Proceedings of the IEEE*, vol. 77, no. 2, pp. 257–286, 1989.

[20] M. Masoum, S. Jamali, and N. Ghaffarzadeh, "Detection and classification of power quality disturbances using discrete wavelet transform and wavelet networks," *IET Science, Measurement & Technology*, vol. 4, no. 4, pp. 193–205, 2010.

[21] T. Abdel-Galil, E. El-Saadany, A. Youssef, and M. Salama, "Disturbance classification using hidden markov models and vector quantization," *Power Delivery, IEEE Transactions on*, vol. 20, no. 3, pp. 2129–2135, 2005.

[22] S. Upadhyaya and S. Mohanty, "Power quality disturbance detection using wavelet based signal processing," in *India Conference (INDICON), 2013 Annual IEEE*, pp. 1–6, IEEE, 2013.

[23] M. Biswal and P. K. Dash, "Measurement and classification of simultaneous power signal patterns with an s-transform variant and fuzzy decision tree," *Industrial Informatics, IEEE Transactions on*, vol. 9, no. 4, pp. 1819–182